Deutsche Forschungsgemeinschaft
Priority Programme 1962

A Novel $W^{1,\infty}$ Approach to Shape Optimisation with Lipschitz Domains

Klaus Deckelnick, Philip J. Herbert, Michael Hinze

SPP 1962
Non-smooth and Complementarity-based Distributed Parameter Systems: Simulation and Hierarchical Optimization

Preprint Number SPP1962-162

received on March 26, 2021

Edited by
SPP1962 at Weierstrass Institute for Applied Analysis and Stochastics (WIAS)
Leibniz Institute in the Forschungsverbund Berlin e.V.
Mohrenstraße 39, 10117 Berlin, Germany
E-Mail: spp1962@wias-berlin.de

World Wide Web: http://spp1962.wias-berlin.de/

A NOVEL $W^{1,\infty}$ APPROACH TO SHAPE OPTIMISATION WITH LIPSCHITZ DOMAINS

KLAUS DECKELNICK, PHILIP J. HERBERT, AND MICHAEL HINZE

Abstract. This article introduces a novel method for the implementation of shape optimisation with Lipschitz domains. We propose to use the shape derivative to determine deformation fields which represent steepest descent directions of the shape functional in the $W^{1,\infty}-$ topology. The idea of our approach is demonstrated for shape optimisation of n-dimensional star-shaped domains, which we represent as functions defined on the unit $(n-1)$-sphere. In this setting we provide the specific form of the shape derivative and prove the existence of solutions to the underlying shape optimisation problem. Moreover, we show the existence of a direction of steepest descent in the $W^{1,\infty}-$ topology. We also note that shape optimisation in this context is closely related to the $\infty-$Laplacian, and to optimal transport, where we highlight the latter in the numerics section. We present several numerical experiments illustrating that our approach seems to be superior over existing Hilbert space methods, in particular in developing optimal shapes with corners.

1. Introduction

In the present work we are interested in the numerical solution of a certain class of shape optimisation problems

$$\min \mathcal{J}(\Omega),\ \Omega \in \mathcal{S},$$

where $\mathcal{S}$ denotes the set of admissible shapes to be specified in the respective application. A common approach in order to calculate at least local minima of $\mathcal{J}$ consists in applying the steepest descent method to the shape derivative of $\mathcal{J}$. More precisely, given a shape $\Omega \in \mathcal{S}$, one determines a descent vector field $V^* : \mathbb{R}^n \to \mathbb{R}^n$ satisfying $\mathcal{J}'(\Omega)(V^*) < 0$ and sets $\Omega_{\text{new}} := (\text{id} + \alpha V^*)(\Omega)$ for a suitable step size $\alpha > 0$. A common approach in order to determine a descent direction V^* employs a Hilbert space setting. Let H be a Hilbert space with scalar product $a(\cdot, \cdot)$, then V is determined by minimising

$$V \mapsto a(V, V) + \mathcal{J}'(\Omega)(V), V \in H.$$

A nice discussion of the pros and cons of this approach can be found in Section 5.2 of [ADJ21]. Typical choices of H are the Sobolev spaces $H^m(\mathbb{R}^n; \mathbb{R}^n)$, where one however needs to choose m sufficiently large in order to obtain a Lipschitz transformation. A way around this restriction is to leave the Hilbertian framework and to consider for $p \geq 2$ the regularisation

$$V \mapsto \frac{1}{p} \int |DV|^p + \mathcal{J}'(\Omega)(V)$$

Date: March 26, 2021.

as well as the limit $p \to \infty$. A problem of this type has been studied by Ishii and Loreti in [IL05] starting from the the p-Laplace relaxed problem

$$v_p = \underset{v \in W_0^{1,p}(\Omega)}{\arg\max}\; I_p(v) := \int_\Omega f(x)v(x) - \frac{1}{p}|\nabla v(x)|^p \mathrm{d}x.$$

Here $f \in C(\bar{\Omega})$ is given. It is shown that under certain conditions the sequence $(v_p)_{p>1}$ converges uniformly to a solution $v^* \in W_0^{1,\infty}(\Omega)$ of the variational problem

$$v^* = \underset{\{v \in W_0^{1,\infty}(\Omega), \|\nabla v\|_\infty \leq 1\}}{\arg\max} I_\infty(v) := \int_\Omega f(x)v(x)\mathrm{d}x.$$

In addition, [IL05, Theorem 2.1] gives an explicit formula for v^* in the case $\Omega = (0, a) \subset \mathbb{R}$. Our aim is to apply the above ideas and results in the context of shape optimisation in order to determine descent directions in the $W^{1,\infty}-$topology. To do so, we shall focus on the case that the admissible domains $\Omega \subset \mathbb{R}^n$ are starshaped with respect to the origin so that shapes and their perturbations can be described in terms of scalar functions $f : \mathbb{S}^{n-1} = \{x \in \mathbb{R}^n \,|\, |x| = 1\} \to \mathbb{R}$. In this setting we consider the following model problem

$$\inf_{\Omega \in \mathcal{S}} \mathcal{J}(\Omega) := \frac{1}{2}\int_\Omega |u_\Omega - z|^2 \mathrm{d}x, \tag{1}$$

where $u_\Omega \in H_0^1(\Omega)$ is the unique weak solution of

$$\int_\Omega \nabla u \cdot \nabla \eta \,\mathrm{d}x = \int_\Omega F\,\eta\,\mathrm{d}x \qquad \forall \eta \in H_0^1(\Omega) \tag{2}$$

and $z \in H^1(D)$, $F \in L^2(D)$ are given functions on some hold–all domain D. In Section 2 we reformulate (1), (2) as a minimisation problem on a suitable subset of $W^{1,\infty}(\mathbb{S}^{n-1})$ and calculate the shape derivative in terms of the solution of the state and adjoint equation. Furthermore, we prove the existence of an optimal Lipschitz–continuous descent direction, for which we derive an explicit formula in the case $n = 2$. Using a discrete version of this formula together with finite element discretisations of the state and adjoint equation we obtain an appoximation of the optimal descent direction which is used in the steepest descent method. The numerical experiments shown in Section 4 demonstrate that this novel approach performs better than methods relying on H^1–regularisation. Let us also mention that our approach is related to optimal transport, see [San15].

There exists a vast amount of literature related to shape optimisation problems. We first mention the seminal works of Delfour and Zolésio [DZ01], of Sokolowski and Zolésio [SZ92], and the recent overview article [ADJ21] by Allaire, Dapogny, and Jouve, where also a comprehensive bibliography on the topic can be found. The mathematical and numerical analysis of shape optimisation problems has a long history, see e.g. [Bel+97; GM94; MS76; Sim80]. With increasing computing power, shape optimisation has experienced a renaissance in recent years [SSW15; SSW16; SW17], especially in fluid mechanical applications [Bra+15; Fis+17; Gar+15; Gar+18; Rad+18; HUU20; HSUar; Küh+19; Sch+13]. A steepest descent method for the numerical solution utilising a Hilbert-space framework for PDE constrained shape optimisation is investigated in [HP15]. A comparison of numerical approximations of Hilbertian shape gradients in boundary and volume form is presented in [HPS15].

Finally we recall that an extensive summary of the state of the art in numerical approaches to shape and topology optimisation is given in [ADJ21, Chapter 6-9].

2. Analysis of a model problem

2.1. **Reformulation and existence of a minimum.** Let us begin by introducing some notation: a bounded domain $\Omega \subset \mathbb{R}^n$ is called star–shaped with respect to the origin if $[0, x] \subset \Omega$ for every $x \in \Omega$. Furthermore, Ω is called star–shaped with respect to $B_\epsilon(0)$ if $[y, x] \subset \Omega$ for every $y \in B_\epsilon(0)$ and every $x \in \Omega$. For a bounded domain Ω that is star–shaped with respect to the origin we denote by $f_\Omega : \mathbb{S}^{n-1} \to \mathbb{R}_{>0}$ its radial function given by

$$f_\Omega(\omega) := \sup\{\lambda > 0 \,|\, \lambda\omega \in \Omega\}, \quad \omega \in \mathbb{S}^{n-1}. \tag{3}$$

It is shown in [Bur98, Lemma 2, Section 3.2] that Ω is star–shaped with respect to a ball $B_\epsilon(0)$ if and only if f_Ω is Lipschitz–continuous on $\mathbb{S}^{n-1}$. Conversely, a positive, Lipschitz–continuous function $f : \mathbb{S}^{n-1} \to \mathbb{R}$ defines a bounded domain that is star–shaped with respect to the origin via

$$\Omega_f := \{x \in \mathbb{R}^n \,|\, x = 0 \text{ or } |x| < f(\omega_x), x \neq 0\}, \quad \text{where } \omega_x = \frac{x}{|x|}. \tag{4}$$

We will be using Lebesgue and Sobolev spaces on $\mathbb{S}^{n-1}$, equipped with the $(n-1)$-dimensional Hausdorff measure on $\mathbb{S}^{n-1}$. Since $C^{0,1}(\mathbb{S}^{n-1}) = W^{1,\infty}(\mathbb{S}^{n-1})$, the tangential gradient $\nabla_T f$ is defined almost everywhere on $\mathbb{S}^{n-1}$. We give the explicit definition of the tangential gradient by its definition on charts. Let $\Theta \subset \mathbb{R}^{n-1}$ be open and bounded and $X\colon \Theta \to \mathbb{S}^{n-1}$ be a C^2-diffeomorphism onto its image, $U := X(\Theta)$. Then, for almost every $\omega \in U$,

$$\nabla_T f(\omega) := \left(\sum_{i,j=1}^{n-1} g^{ij} \frac{\partial(f \circ X)}{\partial\theta_j} \frac{\partial X}{\partial\theta_j}\right) \circ X^{-1}(\omega),$$

where $\{\theta_i\}_{i=1}^{n-1}$ are an orthonormal coordinate frame on Θ and g^{ij} is the ij element of the inverse matrix of G, which has elements $g_{ij} = \frac{\partial X}{\partial\theta_i} \cdot \frac{\partial X}{\partial\theta_j}$ for $i, j = 1, ..., n-1$. For more details on this parametric representation, see [DDE05], in particular equation (2.14). We note that this definition is independent of the paramaterisation X as well as

$$\nabla_T f \in L^\infty(\mathbb{S}^{n-1}), \quad \nabla_T f(\omega) \cdot \omega = 0 \text{ a.e. on } \mathbb{S}^{n-1}. \tag{5}$$

Lemma 2.1. *Let $f \in W^{1,\infty}(\mathbb{S}^{n-1})$ with $f_0 := \min_{\omega\in\mathbb{S}^{n-1}} f(\omega) > 0$ and $L := \|\nabla_T f\|_{L^\infty(\mathbb{S}^{n-1})}$. Then:*

(i) Ω_f is star–shaped with respect to $B_\epsilon(0)$, where $\epsilon = \frac{2}{\pi}\frac{f_0^2}{\sqrt{L^2+f_0^2}}$.

(ii) Let $\Phi_f : \mathbb{R}^n \to \mathbb{R}^n$ be defined by

$$\Phi_f(x) := \begin{cases} f(\omega_x)x, & x \neq 0, \\ 0, & x = 0. \end{cases} \tag{6}$$

Then Φ_f is bi–Lipschitz with $\Phi_f(B) = \Omega_f$, where $B = \{x \in \mathbb{R}^n \,|\, |x| < 1\}$. In addition

$$D\Phi_f(x) = f(\omega_x)I + \omega_x \otimes \nabla_T f(\omega_x) \quad \text{and} \quad \det D\Phi_f(x) = f(\omega_x)^n \quad \text{a.e. in } B, \tag{7}$$

where $(a \otimes b)_{ij} := a_i b_j$ for vectors $a, b \in \mathbb{R}^n$.

Proof. (i) Clearly, f is the radial function for Ω_f. Let $\omega_1, \omega_2 \in \mathbb{S}^{n-1}$ and $\eta : [0,1] \to \mathbb{S}^{n-1}$ a curve with $\eta(0) = \omega_1, \eta(1) = \omega_2$ and $\int_0^1 |\eta'(t)|\,\mathrm{d}t = d(\omega_1, \omega_2)$, where $d(\cdot,\cdot)$ denotes the spherical metric on $\mathbb{S}^{n-1}$. Assuming that $f \in C^1(\mathbb{S}^{n-1})$ for a moment we have

$$|f(\omega_2) - f(\omega_1)| = |\int_0^1 \frac{d}{dt}(f \circ \eta)(t)\mathrm{d}t| = |\int_0^1 \nabla_T f(\gamma(t)) \cdot \eta'(t)\mathrm{d}t| \leq L d(\omega_1, \omega_2).$$

Applying this estimate to a suitable regularisation of f yields the same bound in the general case. The fact that Ω_f is star–shaped with respect to $B_\epsilon(0)$ with ϵ as given above now follows from the proof of [Bur98, Lemma 2, Section 3.2], see in particular p. 97.
(ii) Since $f(\omega) \geq f_0, \omega \in \mathbb{S}^{n-1}$ it is straightforward to verify that Φ_f is bi–Lipschitz with $\Phi_f(B) = \Omega_f$. Furthermore,

$$D\Phi_f(x) = f(\omega_x)I + \omega_x \otimes P(x)\nabla_T f(\omega_x),$$

where $P(x) := I - \omega_x \otimes \omega_x$. Observing that $\nabla_T f(\omega_x) \cdot x = 0$ by (5) gives that $P(x)\nabla_T f(\omega_x) = \nabla_T f(\omega_x)$ to conclude the form of $D\Phi_f$. Using that $\omega_x \otimes \nabla_T f(\omega_x)$ is a rank 1 term with vanishing trace, we deduce (7). ☐

Using (7) together with the transformation rule we infer that

$$|\Omega_f| = \int_B |\mathrm{det} D\Phi_f(x)|\,\mathrm{d}x = \int_0^1 \int_{\mathbb{S}^{n-1}} f(\omega)^n \mathrm{d}o_\omega r^{n-1}\mathrm{d}r = \frac{1}{n}\int_{\mathbb{S}^{n-1}} f(\omega)^n \mathrm{d}o_\omega. \tag{8}$$

Let us fix $\rho > 0, L > 0$ and $\gamma > 0$ with $\gamma > \rho^n |\mathbb{S}^{n-1}|$. We define

$$\begin{aligned} \mathcal{F} := \{ f \in W^{1,\infty}(\mathbb{S}^{n-1}) \,|\, f \geq \rho \text{ in } \mathbb{S}^{n-1}, \\ \|\nabla_T f\|_{L^\infty(\mathbb{S}^{n-1})} \leq L, \int_{\mathbb{S}^{n-1}} f(\omega)^n \mathrm{d}o_\omega = \gamma \}. \end{aligned} \tag{9}$$

Note that if $f \in \mathcal{F}$, then there exists $\bar{\omega} \in \mathbb{S}^{n-1}$ such that $f(\bar{\omega})^n |\mathbb{S}^{n-1}| = \gamma$. Hence we obtain for every $\omega \in \mathbb{S}^{n-1}$ that

$$f(\omega) \leq f(\bar{\omega}) + L d(\omega, \bar{\omega}) \leq \left(|\mathbb{S}^{n-1}|^{-1}\gamma\right)^{\frac{1}{n}} + \pi L := R,$$

so that all sets Ω_f given by (4) are contained in the hold–all domain $D = B_R(0)$. We now define

$$J : \mathcal{F} \to \mathbb{R},\ J(f) := \mathcal{J}(\Omega_f) = \frac{1}{2}\int_{\Omega_f} |u - z|^2 \mathrm{d}x,$$

where $u \in H_0^1(\Omega_f)$ solves

$$\int_{\Omega_f} \nabla u \cdot \nabla \eta \,\mathrm{d}x = \int_{\Omega_f} F\,\eta\,\mathrm{d}x \qquad \forall \eta \in H_0^1(\Omega_f). \tag{10}$$

Hence we consider the optimisation problem (1), (2) in the class $\mathcal{S} = \{\Omega_f \,|\, f \in \mathcal{F}\}$. In view of Lemma 2.1 and (8) the class of admissible domains comprises of bounded domains of fixed volume, which contain $B_\rho(0)$ and which are star–shaped with respect to $B_\epsilon(0)$, where $\epsilon = \frac{2}{\pi}\frac{\rho^2}{\sqrt{L^2+\rho^2}}$. Let us next establish the existence of a solution of the resulting optimisation problem.

Theorem 2.2. *There exists $f_* \in \mathcal{F}$ such that $J(f_*) = \min_{f \in \mathcal{F}} J(f)$.*

Proof. Since $\gamma > \rho^n|\mathbb{S}^{n-1}|$, the function $f \equiv \big(|\mathbb{S}^{n-1}|^{-1}\gamma\big)^{\frac{1}{n}}$ belongs to $\mathcal{F}$, so that $\mathcal{F}$ is non–empty. Let $(f_k)_{k\in\mathbb{N}} \subset \mathcal{F}$ be a sequence such that $J(f_k) \searrow \inf_{f\in\mathcal{F}} J(f)$. By standard compactness results there exists a subsequence, again denoted by $(f_k)_{k\in\mathbb{N}}$ and $f_* \in W^{1,\infty}(\mathbb{S}^{n-1})$ such that

$$f_k \to f_* \text{ in } C(\mathbb{S}^{n-1}) \text{ and } \nabla_T f_k \overset{*}{\rightharpoonup} \nabla_T f_* \text{ in } L^\infty(\mathbb{S}^{n-1}).$$

Clearly, $f_* \in \mathcal{F}$. Let us write $\Omega_k = \Omega_{f_k}$ and $\Omega_* = \Omega_{f_*}$. We claim that $\Omega_k \to \Omega_*$ in the Hausdorff complementary metric, i.e. $d_{\complement\Omega_k} \to d_{\complement\Omega_*}$ in $C(\bar{D})$, where d_A denotes the distance function to the set A and $\complement A$ its complement. In order to prove the claim we fix $x \in \bar{D}$ and choose $z \in \complement\Omega_*$ such that $d_{\complement\Omega_*}(x) = |x-z|$. Then $R \geq |z| \geq f_*(\omega_z) \geq \rho$. For $z_k = \big(1+\rho^{-1}\|f_k - f_*\|_{L^\infty(\mathbb{S}^{n-1})}\big)z$ we have $\omega_{z_k} = \omega_z$ and

$$|z_k| = |z| + \frac{|z|}{\rho}\|f_k - f_*\|_{L^\infty(\mathbb{S}^{n-1})} \geq f_*(\omega_z) + \|f_k - f_*\|_{L^\infty(\mathbb{S}^{n-1})} \geq f_k(\omega_z) = f_k(\omega_{z_k}).$$

Therefore, $z_k \in \complement\Omega_k$ so that

$$\begin{aligned} d_{\complement\Omega_k}(x) - d_{\complement\Omega_*}(x) &\leq |x-z_k| - |x-z| \leq |z_k - z| = \\ &= \frac{|z|}{\rho}\|f_k - f_*\|_{L^\infty(\mathbb{S}^{n-1})} \leq \frac{R}{\rho}\|f_k - f_*\|_{L^\infty(\mathbb{S}^{n-1})}. \end{aligned}$$

By exchanging the roles of f_k and f_* and taking the maximum with respect to x we obtain

$$\max_{x\in\bar{D}} |d_{\complement\Omega_k}(x) - d_{\complement\Omega_*}(x)| \leq \frac{R}{\rho}\|f_k - f_*\|_{L^\infty(\mathbb{S}^{n-1})} \to 0,\ k \to \infty,$$

which has shown $\Omega_k \to \Omega_*$ in the Hausdorff complementary metric. Furthermore, according to [Bur98, Lemma 3, Section 3.2] the set Ω_* satisfies the cone condition and hence is locally Lipschitz. We may therefore deduce from Theorem 4.1 in Chapter 6 of [DZ01] that $u_{\Omega_k} \to u_{\Omega_*}$ in $H_0^1(D)$. As a result $J(f_*) = \lim_{k\to\infty} J(f_k) = \inf_{f\in\mathcal{F}} J(f)$ which completes the proof. ∎

2.2. **Calculating the shape derivative.** Let $F \in L^2_{loc}(\mathbb{R}^n), z \in H^1_{loc}(\mathbb{R}^n)$, and let us fix

$$f \in W^{1,\infty}(\mathbb{S}^{n-1}) \text{ with } \min_{\omega\in\mathbb{S}^{n-1}} f(\omega) > 0.$$

Before we calculate a formula for the directional derivative of J at f we transform the state equation to the reference domain B. To do so, define $\hat{u}(x) := u(\Phi_f(x))$, where $u \in H_0^1(\Omega_f)$ denotes the solution of (10) and Φ_f is given by (6). Clearly, $\nabla u(\Phi_f(x)) = D\Phi_f(x)^{-t}\,\nabla\hat{u}(x)$, where we think of the gradient as a column vector. Therefore, (10) translates into

$$\int_B A_f(\omega_x)\nabla\hat{u}(x)\cdot\nabla\hat{\eta}(x)\,\mathrm{d}x = \int_B \hat{F}_f(x)\hat{\eta}(x)\,f(\omega_x)^n\,\mathrm{d}x \quad \forall\,\hat{\eta} \in H_0^1(B). \tag{11}$$

In the above $\hat{F}_f(x) = F(\Phi_f(x))$ and $A_f(\omega_x) = f(\omega_x)^n\,D\Phi_f(x)^{-1}D\Phi_f(x)^{-t}$. Using the fact that

$$D\Phi_f(x)^{-1} = \frac{1}{f(\omega_x)}\Big(I - \omega_x \otimes \frac{\nabla_T f(\omega_x)}{f(\omega_x)}\Big)$$

we find that

$$A_f(\omega_x) = f(\omega_x)^{n-2}\Big(I - \omega_x \otimes \frac{\nabla_T f(\omega_x)}{f(\omega_x)} - \frac{\nabla_T f(\omega_x)}{f(\omega_x)} \otimes \omega_x + \frac{|\nabla_T f(\omega_x)|^2}{f(\omega_x)^2}\,\omega_x \otimes \omega_x\Big). \tag{12}$$

In order to calculate $\langle J'(f), g\rangle$ for a given direction $g \in W^{1,\infty}(\mathbb{S}^{n-1})$ we define the vector–field $V \in C^{0,1}(\mathbb{R}^n;\mathbb{R}^n)$ by

$$V(y) = \begin{cases} \dfrac{g(\omega_y)}{f(\omega_y)} y, & y \neq 0, \\ 0, & y = 0. \end{cases} \tag{13}$$

Then, $(\mathrm{id} + tV)(\Omega_f) = (\mathrm{id} + tV) \circ \Phi_f(B)$. For every $x \in B$ we have

$$\Phi_f(x) + tV(\Phi_f(x)) = \begin{cases} (f(\omega_x) + tg(\omega_x))x, & x \neq 0, \\ 0, & x = 0, \end{cases}$$

so that $(\mathrm{id} + tV)(\Omega_f) = \Omega_{f+tg}$.

Observing that

$$\begin{aligned} \langle J'(f), g\rangle &= \lim_{t\to 0} \frac{J(f+tg) - J(f)}{t} = \\ &= \lim_{t\to 0} \frac{\mathcal{J}((\mathrm{id}+tV)(\Omega_f)) - \mathcal{J}(\Omega_f)}{t} = \mathcal{J}'(\Omega_f)(V), \end{aligned} \tag{14}$$

allows us to apply formulae for $\mathcal{J}'(\Omega_f)(V)$ that are available in the literature. By adapting the proof of [ADJ21, Proposition 4.5] to our situation we obtain the *volume form* of the shape derivative as

$$\begin{aligned} \mathcal{J}'(\Omega_f)(V) \;\; = \;\; & \int_{\Omega_f} \big(DV + DV^t - \mathrm{div}V\, I\big)\nabla u \cdot \nabla p \,\mathrm{d}x \\ & + \int_{\Omega_f} \big(\tfrac{1}{2}(u-z)^2 \,\mathrm{div}V - (u-z)\nabla z \cdot V\big)\,\mathrm{d}x - \int_{\Omega_f} FV \cdot \nabla p \,\mathrm{d}x. \end{aligned} \tag{15}$$

The *boundary form* of the shape derivative – under appropriate regularity assumptions on u and p – can be written down in the form

$$\mathcal{J}'(\Omega_f)(V) = \int_{\partial\Omega_f} \left(\frac{1}{2}(u-z)^2 + \frac{\partial u}{\partial \nu}\frac{\partial p}{\partial \nu}\right) V \cdot \nu \,\mathrm{d}S, \tag{16}$$

where ν is almost everywhere the outward unit normal to Ω_f, compare [ADJ21, Theorem 4.6]. Here $p \in H^1_0(\Omega_f)$ is the solution of the adjoint problem

$$\int_{\Omega_f} \nabla p \cdot \nabla \eta \,\mathrm{d}x = \int_{\Omega_f} (u-z)\eta \,\mathrm{d}x \qquad \forall \eta \in H^1_0(\Omega_f). \tag{17}$$

Transforming the volume form (15) to the reference domain B. By (14) we have

$$\begin{aligned} \langle J'(f), g\rangle = & \int_B (D\Phi_f)^{-1}\big(DV + DV^t - (\mathrm{div}V)\, I\big) \circ \Phi_f (D\Phi_f)^{-t} \nabla\hat{u} \cdot \nabla\hat{p}\, f(\omega_x)^n \,\mathrm{d}x \\ & + \int_B \big(\tfrac{1}{2}(\hat{u} - \hat{z}_f)^2 \,(\mathrm{div}V) \circ \Phi_f - (\hat{u} - \hat{z}_f)\nabla\hat{z}_f \cdot (D\Phi_f)^{-1} V \circ \Phi_f\big) f(\omega_x)^n \,\mathrm{d}x \\ & - \int_B \hat{F}_f (D\Phi_f)^{-1} V \circ \Phi_f \cdot \nabla\hat{p}\, f(\omega_x)^n \,\mathrm{d}x, \end{aligned} \tag{18}$$

where $\hat{z}_f(x) = z(\Phi_f(x))$. In the same way as above we obtain from (17) that $\hat{p}(x) = p(\Phi_f(x))$ satisfies

$$\int_B A_f(\omega_x)\nabla\hat{p}(x) \cdot \nabla\hat{\eta}(x)\,\mathrm{d}x = \int_B (\hat{u}(x) - \hat{z}_f(x))\hat{\eta}(x)\, f(\omega_x)^n \,\mathrm{d}x \;\; \forall\, \hat{\eta} \in H^1_0(B). \tag{19}$$

Differentiating the relation $V(\Phi_f(x)) = g(\omega_x)x$ we obtain

$$DV(\Phi_f(x))D\Phi_f(x) = g(\omega_x)I + \omega_x \otimes \nabla_T g(\omega_x)$$

and hence

$$DV \circ \Phi_f = \big(gI + \omega_x \otimes \nabla_T g\big)(D\Phi_f)^{-1} = \frac{1}{f}\big(gI - \frac{g}{f}\,\omega_x \otimes \nabla_T f + \omega_x \otimes \nabla_T g\big).$$

In particular we deduce that

$$(\mathrm{div} V) \circ \Phi_f = \mathrm{trace}\, DV \circ \Phi_f = n\frac{g}{f}$$

as well as

$$\begin{aligned} & DV \circ \Phi_f + DV^t \circ \Phi_f - \mathrm{div} V \circ \Phi_f \, I \\ = \quad & \frac{g}{f}(2-n)I - \frac{g}{f^2}\omega_x \otimes \nabla_T f - \frac{g}{f^2}\nabla_T f \otimes \omega_x + \frac{1}{f}\omega_x \otimes \nabla_T g + \frac{1}{f}\nabla_T g \otimes \omega_x. \end{aligned}$$

A long, but straightforward calculation then shows that

$$\begin{aligned} & (D\Phi_f)^{-1}\big(DV \circ \Phi_f + DV^t \circ \Phi_f - \mathrm{div} V \circ \Phi_f \, I\big)(D\Phi_f)^{-t} \\ = \quad & \frac{g}{f^3}(2-n)I + (n-3)\frac{g}{f^4}\big(\omega_x \otimes \nabla_T f + \nabla_T f \otimes \omega_x\big) + \frac{1}{f^3}\big(\omega_x \otimes \nabla_T g + \nabla_T g \otimes \omega_x\big) \\ & + \big((4-n)\frac{g}{f^5}|\nabla_T f|^2 - 2\frac{1}{f^4}\big(\nabla_T f \cdot \nabla_T g\big)\big)\omega_x \otimes \omega_x. \end{aligned}$$

Note also that

$$(D\Phi_f)^{-1} V \circ \Phi_f = \frac{1}{f}\big(I - \omega_x \otimes \frac{\nabla_T f}{f}\big)gx = \frac{g}{f}x = |x|\frac{g}{f}\omega_x.$$

If we insert the above identities into (18) and transform to polar coordinates we obtain

$$\langle J'(f), g\rangle = \int_B \big(h_f g + H_f \cdot \nabla_T g\big)\mathrm{d}x = \int_{\mathbb{S}^{n-1}} \big(\tilde{h}_f g + \tilde{H}_f \cdot \nabla_T g\big) do_\omega, \tag{20}$$

where $h_f : B \to \mathbb{R}$ and $H_f : B \to \mathbb{R}^n$ are defined by

$$\begin{aligned} (21)\; h_f \quad = \quad & (2-n)f^{n-3}\nabla\hat{u} \cdot \nabla\hat{p} + (4-n)f^{n-5}|\nabla_T f|^2(\nabla\hat{u} \cdot \omega_x)(\nabla\hat{p} \cdot \omega_x) \\ & + (n-3)f^{n-4}\big((\nabla_T f \cdot \nabla\hat{u})(\omega_x \cdot \nabla\hat{p}) + (\nabla_T f \cdot \nabla\hat{p})(\omega_x \cdot \nabla\hat{u})\big) \\ & + f^{n-1}\big(\frac{n}{2}(\hat{u} - \hat{z}_f)^2 - |x|(\hat{u} - \hat{z}_f)\nabla\hat{z}_f \cdot \omega_x - |x|\hat{F}_f\, \nabla\hat{p} \cdot \omega_x\big); \\ (22) H_f \quad = \quad & f^{n-3}\big((\nabla\hat{p} \cdot \omega_x)\nabla\hat{u} + (\nabla\hat{u} \cdot \omega_x)\nabla\hat{p}\big) - 2f^{n-4}(\nabla\hat{u} \cdot \omega_x)(\nabla\hat{p} \cdot \omega_x)\, \nabla_T f, \end{aligned}$$

while $\tilde{h}_f : \mathbb{S}^{n-1} \to \mathbb{R}$, $\tilde{H}_f : \mathbb{S}^{n-1} \to \mathbb{R}^n$ are given by

$$\tilde{h}_f(\omega) = \int_0^1 s^{n-1} h_f(s\omega)\mathrm{d}s, \;\; \tilde{H}_f(\omega) = \int_0^1 s^{n-1} H_f(s\omega)\mathrm{d}s.$$

From our assumptions on z and f we deduce that $\tilde{h}_f \in L^1(\mathbb{S}^{n-1})$, $\tilde{H}_f \in L^1(\mathbb{S}^{n-1}; \mathbb{R}^n)$.

Transforming the boundary form of the shape derivative to $\mathbb{S}^{n-1}$. As we intend to use formula (16) also for numerical purposes we transform it to an integral over the reference boundary $\mathbb{S}^{n-1}$ with the help of the mapping

$$\Phi_{f|\mathbb{S}^{n-1}} : \mathbb{S}^{n-1} \to \partial\Omega_f,\ \omega \mapsto f(\omega)\omega.$$

A calculation shows that

$$\mathrm{d}S = f(\omega)^{n-1}\left(1+\frac{|\nabla_T f(\omega)|^2}{f(\omega)^2}\right)^{1/2}\mathrm{d}o_\omega, \tag{23}$$

while

$$(\nu\circ\Phi_f)(\omega) = \frac{(D\Phi_f(\omega))^{-t}\omega}{|(D\Phi_f(\omega))^{-t}\omega|} = \left(1+\frac{|\nabla_T f(\omega)|^2}{f(\omega)^2}\right)^{-\frac{1}{2}}\big(\omega - \frac{\nabla_T f(\omega)}{f(\omega)}\big).$$

Since $(\nabla u\circ\Phi_f)(\omega) = (D\Phi_f(\omega))^{-t}\nabla\hat{u}(\omega)$ we deduce that

$$\begin{aligned}\frac{\partial u}{\partial\nu}\circ\Phi_f &= \left(1+\frac{|\nabla_T f|^2}{f^2}\right)^{-\frac{1}{2}}(D\Phi_f)^{-t}\nabla\hat{u}\cdot\big(\omega-\frac{\nabla_T f}{f}\big)\\ &= \frac{1}{f}\left(1+\frac{|\nabla_T f|^2}{f^2}\right)^{-\frac{1}{2}}\big(I-\frac{\nabla_T f}{f}\otimes\omega\big)\nabla\hat{u}\cdot\big(\omega-\frac{\nabla_T f}{f}\big)\\ &= \frac{1}{f}\left(1+\frac{|\nabla_T f|^2}{f^2}\right)^{\frac{1}{2}}\frac{\partial\hat{u}}{\partial\omega},\end{aligned}$$

where we have used that $\nabla\hat{u}\cdot\nabla_T f = 0$ on ∂B since $\hat{u}=0$ on ∂B. For the function V given by (13) we have $(V\circ\Phi_f)(\omega) = g(\omega)\omega$ and hence by (5)

$$(V\cdot\nu)\circ\Phi_f = \left(1+\frac{|\nabla_T f|^2}{f^2}\right)^{-\frac{1}{2}} g.$$

After applying the transformation rule to (16), using (23) as well as the formulae above we find

$$\begin{aligned}\langle J'(f),g\rangle &= \int_{\mathbb{S}^{n-1}}\left(\frac{1}{2}(\hat{u}-\hat{z}_f)^2 + (\frac{\partial u}{\partial\nu}\frac{\partial p}{\partial\nu})\circ\Phi_f\right)(V\cdot\nu)\circ\Phi_f\, f^{n-1}\left(1+\frac{|\nabla_T f|^2}{f^2}\right)^{\frac{1}{2}}\mathrm{d}o_\omega\\ &= \int_{\mathbb{S}^{n-1}}\tilde{h}_f g\,\mathrm{d}o_\omega,\end{aligned}$$

where $\tilde{h}_f : \mathbb{S}^{n-1}\to\mathbb{R}$ is given by

$$\tilde{h}_f(\omega) = \frac{1}{2}(\hat{u}(\omega)-\hat{z}_f(\omega))^2 f(\omega)^{n-1} + f(\omega)^{n-3}\big(1+\frac{|\nabla_T f(\omega)|^2}{f(\omega)^2}\big)\frac{\partial\hat{u}}{\partial\omega}(\omega)\frac{\partial\hat{p}}{\partial\omega}(\omega). \tag{24}$$

In the case that u and p are regular enough to ensure that $\tilde{h}_f\in L^1(\mathbb{S}^{n-1})$ the existence of an optimal descent direction will be given in Theorem 2.3 with $\tilde{H}_f\equiv 0$.

A descent direction in the $W^{1,\infty}-$ topology. The volume constraint

$$\int_{\mathbb{S}^{n-1}} f(\omega)^n\mathrm{d}o_\omega = \gamma$$

in the definition of $\mathcal{F}$ in (9) gives rise to the condition $\int_{\mathbb{S}^{n-1}} f^{n-1}g\,\mathrm{d}o_\omega = 0$ for feasible perturbations g of f. We therefore introduce the following set of admissible directions

$$V_\infty(f) \quad := \quad \left\{ v \in W^{1,\infty}(\mathbb{S}^{n-1}) \,:\, \int_{\mathbb{S}^{n-1}} f^{n-1} v \,\mathrm{d}o_\omega = 0,\ \|\nabla_T v\|_{L^\infty(\mathbb{S}^{n-1})} \leq 1 \right\}.$$

Theorem 2.3. *Let $f \in W^{1,\infty}(\mathbb{S}^{n-1})$ with $\min_{\omega \in \mathbb{S}^{n-1}} f(\omega) > 0$. There exists $g \in V_\infty(f)$ such that $\langle J'(f), g\rangle = \min_{v \in V_\infty(f)} \langle J'(f), v\rangle$.*

Proof. In view of (20) we have $\langle J'(f), v\rangle = I_\infty(v)$ with

$$I_\infty(v) := \int_{\mathbb{S}^{n-1}} \big(\tilde{h}_f v + \tilde{H}_f \cdot \nabla_T v\big) \mathrm{d}o_\omega.$$

Step 1: We first prove the result under the stronger condition that $\tilde{h}_f \in L^\infty(\mathbb{S}^{n-1})$, $\tilde{H}_f \in W^{1,\infty}(\mathbb{S}^{n-1};\mathbb{R}^n)$ so that $\tilde{h}_f - \nabla_T \cdot \tilde{H}_f + (n-1)\tilde{H}_f \cdot \omega - c f^{n-1} \in L^\infty(\mathbb{S}^{n-1})$. We obtain after integration by parts on $\mathbb{S}^{n-1}$ that

$$I_\infty(v) = \int_{\mathbb{S}^{n-1}} \big(\tilde{h}_f - \nabla_T \cdot \tilde{H}_f + (n-1)\tilde{H}_f \cdot \omega - c f^{n-1}\big) v \mathrm{d}o_\omega, \quad v \in V_\infty(f)$$

where

$$c = \Big(\int_{\mathbb{S}^{n-1}} f^{n-1} \mathrm{d}o_\omega\Big)^{-1} \int_{\mathbb{S}^{n-1}} \big(\tilde{h}_f - \nabla_T \cdot \tilde{H}_f + (n-1)\tilde{H}_f \cdot \omega\big) \mathrm{d}o_\omega.$$

We note that the $(n-1)\tilde{H}_f \cdot \omega$ term arises from the mean curvature of $\mathbb{S}^{n-1}$, see [DDE05, Equation (2.16)] for example. If we let $q_f := \tilde{h}_f - \nabla_T \cdot \tilde{H}_f + (n-1)\tilde{H}_f \cdot \omega - c f^{n-1}$ we have

$$I_\infty(v) = \int_{\mathbb{S}^{n-1}} q_f v \mathrm{d}o_\omega, \quad v \in V_\infty(f), \quad \text{with } \int_{\mathbb{S}^{n-1}} q_f \mathrm{d}o_\omega = 0.$$

By adapting the arguments in [IL05, Section 5] to our setting, a solution $g \in V_\infty(f)$ with $I_\infty(g) = \min_{v \in V_\infty(f)} I_\infty(v)$ can be obtained as the uniform limit of the sequence $(g_p)_{p>2}$ solving the variational problems

$$\min\{\frac{1}{p} \int_{\mathbb{S}^{n-1}} |\nabla_T v|^p \mathrm{d}o_\omega - \int_{\mathbb{S}^{n-1}} q_f v \mathrm{d}o_\omega \,|\, v \in W^{1,p}(\mathbb{S}^{n-1}), \int_{\mathbb{S}^{n-1}} f^{n-1} v \mathrm{d}o_\omega = 0\}.$$

The estimate on p. 426 in [IL05] requires Poincaré's inequality in $W^{1,1}(\mathbb{S}^{n-1})$ which is available in our case.
Step 2: In the general case there exist sequences $(h_k)_{k\in\mathbb{N}} \subset L^\infty(\mathbb{S}^{n-1})$, $(H_k)_{k\in\mathbb{N}} \subset W^{1,\infty}(\mathbb{S}^{n-1};\mathbb{R}^n)$ such that $h_k \to \tilde{h}_f$ in $L^1(\mathbb{S}^{n-1})$ and $H_k \to \tilde{H}_f$ in $L^1(\mathbb{S}^{n-1}, \mathbb{R}^n)$. Let

$$I_k(v) := \int_{\mathbb{S}^{n-1}} \big(h_k v + H_k \cdot \nabla_T v\big) \mathrm{d}o_\omega, \quad k \in \mathbb{N}.$$

It follows from Step 1, that for every $k \in \mathbb{N}$ there is $g_k \in V_\infty(f)$ such that $I_k(g_k) = \min_{v \in V_\infty(f)} I_k(v)$. Furthermore, there is a subsequence $(g_{k_j})_{j\in\mathbb{N}}$ and $g \in W^{1,\infty}(\mathbb{S}^{n-1})$ such that

$$g_{k_j} \to g \text{ in } C(\mathbb{S}^{n-1}) \text{ and } \nabla_T g_{k_j} \overset{*}{\rightharpoonup} \nabla_T g \text{ in } L^\infty(\mathbb{S}^{n-1}).$$

In particular we have that $g \in V_\infty(f)$. Furthermore, we obtain for any $v \in V_\infty(f)$

$$I_\infty(g) = \lim_{k\to\infty} I_k(g_k) \leq \lim_{k\to\infty} I_k(v) = I_\infty(v),$$

so that $I_\infty(g) = \min_{v \in V_\infty(f)} I_\infty(v)$. $\square$

Remark 2.4. *With the notation used in Step 1 of the proof of Theorem 2.3 the constrained minimisation problem may be seen as the (negative of the) dual problem to the optimal transport problem to find a map which minimises the cost of transporting mass from $q_f^+ \mathrm{do}_\omega$ to $q_f^- \mathrm{do}_\omega$ with cost function*

$$\mathbb{S}^{n-1} \times \mathbb{S}^{n-1} \ni (x, y) \mapsto d(x, y),$$

where d is the intrinsic metric on $\mathbb{S}^{n-1}$. We refer the reader to Section 3.1.1 of [San15], in particular Equation (3.1). This relation will be exploited in Section 3.3 as a method to produce an approximation of a direction of maximal descent.

2.3. **Steepest descent for $n = 2$.** The determination of the minimiser g in Theorem 2.3 is by no means straightforward. In what follows we shall focus on the case $n = 2$ and write $\bar{f}(\phi) = f(e^{i\phi})$ for $f \in W^{1,\infty}(\mathbb{S}^1)$. Since $\nabla_T f(e^{i\phi}) = \bar{f}'(\phi) i e^{i\phi}$ we obtain the following form of (20):

$$\langle J'(f), v\rangle = \int_0^{2\pi} \big(\bar{h}_f(\phi) v(\phi) + \bar{H}_f(\phi) v'(\phi)\big)\, \mathrm{d}\phi, \quad v \in W^{1,\infty}_{\mathrm{per}}(0, 2\pi). \tag{25}$$

Here, $\bar{h}_f(\phi) = \tilde{h}_f(e^{i\phi}), \bar{H}_f(\phi) = \tilde{H}_f(e^{i\phi}) \cdot i e^{i\phi}, \phi \in [0, 2\pi]$. The boundary form of the shape derivative can be treated in the same way by using (24) and setting $\tilde{H}_f \equiv 0$.

In this setting the set of admissible directions becomes

$$V_\infty(f) = \{v \in W^{1,\infty}_{\mathrm{per}}(0, 2\pi) \,|\, \int_0^{2\pi} \bar{f} v \mathrm{d}\phi = 0,\ \|v'\|_{L^\infty(0,2\pi)} \le 1\}.$$

In order to proceed and motivate our numerical approach we assume the situation in Step 1 of the proof of Theorem 2.3, namely that $\bar{H}_f \in W^{1,1}(0, 2\pi)$ with $\bar{H}_f(0) = \bar{H}_f(2\pi)$. Then we obtain after integration by parts and using the condition $\int_0^{2\pi} \bar{f}\, v \mathrm{d}\phi = 0$

$$\langle J'(f), v\rangle = \int_0^{2\pi} (\bar{h}_f(\phi) - \bar{H}_f'(\phi) - c\bar{f}(\phi)) v(\phi) \mathrm{d}\phi, \qquad \text{where } c = \frac{\int_0^{2\pi} \bar{h}_f(\phi)\mathrm{d}\phi}{\int_0^{2\pi} \bar{f}(\phi)\mathrm{d}\phi}.$$

If we let $q_f := \bar{h}_f - \bar{H}_f' - c\bar{f}$ we have

$$\langle J'(f), v\rangle = \int_0^{2\pi} q_f(\phi) v(\phi) \mathrm{d}\phi, \quad v \in V_\infty(f),$$

as well as

$$\int_0^{2\pi} q_f(\phi)\mathrm{d}\phi = \int_0^{2\pi} \bar{h}_f(\phi)\mathrm{d}\phi - c\int_0^{2\pi} \bar{f}(\phi)\mathrm{d}\phi - \bar{H}_f(2\pi) + \bar{H}_f(0) = 0$$

by the choice of c. We can now apply the results of Section 3 in [IL05] (for the case of homogeneous Dirichlet boundary conditions) in order to obtain a function $\tilde{g} \in W^{1,\infty}_0(0, 2\pi)$ with $\|\tilde{g}'\|_{L^\infty(0,2\pi)} \le 1$ satisfying

$$\int_0^{2\pi} q_f(\phi)\tilde{g}(\phi)\mathrm{d}\phi = \max_{v \in W^{1,\infty}_0(0,2\pi), \|v'\|_{L^\infty(0,2\pi)} \le 1} \int_0^{2\pi} q_f(\phi) v(\phi)\mathrm{d}\phi. \tag{26}$$

The function $\tilde{g}$ is obtained as the uniform limit of the sequence $(g_p)_{p>2}$, where g_p solves

$$\begin{aligned} -\frac{d}{dx}\left(|g_p'(x)|^{p-2}g_p'(x)\right) &= q_f \text{ in } (0,2\pi) \\ g_p(0) = g_p(2\pi) &= 0. \end{aligned}$$

By calculating g_p and passing to the limit $p \to \infty$, [IL05] derive an explicit formula for $\tilde{g}$. In order to describe this formula we define

$$G(\phi) := \int_0^{\phi} q_f(t)\mathrm{d}t, \tag{27}$$

as well as

$$\begin{aligned} M(r) &:= |\{\phi \in [0,2\pi) : G(\phi) < r\}|, r \in \mathbb{R};\ \beta := \sup\{r \in \mathbb{R} : M(r) \le \pi\}; && (28)\\ O_\pm &:= \{\phi \in [0,2\pi) : G(\phi) \gtrless \beta\},\ O_0 := \{\phi \in [0,2\pi) : G(\phi) = \beta\}; && (29)\\ k &:= \begin{cases} 0, & |O_0| = 0, \\ \frac{|O_+|-|O_-|}{|O_o|}, & \text{otherwise.} \end{cases} && (30) \end{aligned}$$

Note that since q_f is integrable there are $r_0, r_1 \in \mathbb{R}$ such that $M(r) = 0, r \le r_0$ and $M(r) = 2\pi, r \ge r_1$. The function $\tilde{g}$ then is given explicitly by

$$\tilde{g}(\phi) := \int_0^{\phi} (\chi_{O_-}(t) - \chi_{O_+}(t) + k\chi_{O_o}(t))\mathrm{d}t. \tag{31}$$

Let us use $\tilde{g}$ in order to obtain an explicit direction of steepest descent in our periodic setting.

Proposition 2.5. *Let $\bar{g} : [0,2\pi] \to \mathbb{R}$ be defined by $\bar{g}(\phi) := -\tilde{g}(\phi) + \frac{1}{2\pi}\int_0^{2\pi} \bar{f}\tilde{g}\,\mathrm{d}t$. Then $\bar{g} \in V_\infty(f)$ and $\langle J'(f), \bar{g}\rangle = \min_{v \in V_\infty(f)}\langle J'(f), v\rangle$.*

Proof. It is obvious that $\bar{g}$ belongs to $V_\infty(f)$. If $v \in V_\infty(f)$, then $v(0) - v \in W_0^{1,\infty}(0,2\pi)$ with $\|(v(0)-v)'\|_{L^\infty(0,2\pi)} \le 1$ so that (26) implies

$$\begin{aligned} \langle J'(f), \bar{g}\rangle &= \int_0^{2\pi} (\bar{h}_f - \bar{H}_f')\bar{g}\,\mathrm{d}\phi = \int_0^{2\pi} q_f\bar{g}\,\mathrm{d}\phi = -\int_0^{2\pi} q_f\tilde{g}\,\mathrm{d}\phi \\ &\le -\int_0^{2\pi} q_f(v(0)-v)\,\mathrm{d}\phi = \int_0^{2\pi} q_f v\,\mathrm{d}\phi = \langle J'(f), v\rangle, \end{aligned}$$

where we have used that $\int_0^{2\pi} q_f \mathrm{d}\phi = 0$. ☐

3. Discretisation

3.1. **Approximation of the shape derivative.** We use the above ideas in order to set up numerical schemes in two space dimensions. To do so, we approximate both the radial function and the solutions of the state and ajoint equations with the help of continuous, piecewise linear finite elements, but on grids that are independent of each other. Let $\mathcal{T}_h$ be a quasi-uniform triangulation of (a subset of) the unit ball B, where $B_h := \left(\bigcup_{T\in\mathcal{T}_h} T\right)^\circ \subset B$ and the vertices on ∂B_h lie on ∂B. We define $\mathcal{S}_h$ to be

$$\mathcal{S}_h := \{\hat{\eta}_h \in C(B_h)\,|\,\hat{\eta}_h = 0 \text{ on } \partial B_h,\ \hat{\eta}_{h|T} \in P^1(T),\ T \in \mathcal{T}_h\}.$$

Next, given $N \in \mathbb{N}$, we set $\phi_i = 2\pi\frac{i}{N}, i = 0,\dots,N$ as well as

$$\mathcal{S}^N := \{\bar{v} \in C([0,2\pi]) : \bar{v}_{|[\phi_{i-1},\phi_i]} \in P^1([\phi_{i-1},\phi_i]), i = 1,\dots,N, \bar{v}(0) = \bar{v}(2\pi)\},$$

the set of continuous, piecewise linear, periodic functions on $[0, 2\pi]$.
Given $\bar{f} \in \mathcal{S}^N$, we set $f(\omega) = \bar{f}(\phi)$ if $\omega = e^{i\phi}$ and define $\hat{u}_h, \hat{p}_h \in \mathcal{S}_h$ as the unique solutions of

$$\int_{B_h} A_f(\omega_x)\nabla \hat{u}_h \cdot \nabla \hat{\eta}_h \,\mathrm{d}x = \int_{B_h} \hat{F}_f \hat{\eta}_h\, f(\omega_x)^2 \,\mathrm{d}x; \quad \forall \hat{\eta}_h \in \mathcal{S}_h, \tag{32}$$

$$\int_{B_h} A_f(\omega_x)\nabla \hat{p}_h \cdot \nabla \hat{\eta}_h \,\mathrm{d}x = \int_{B_h} (\hat{u}_h - \hat{z}_f)\hat{\eta}_h\, f(\omega_x)^2 \,\mathrm{d}x \quad \forall \hat{\eta}_h \in \mathcal{S}_h, \tag{33}$$

where the integrals are calculated with quadrature. Let us use $\hat{u}_h$ and $\hat{p}_h$ in order to define discrete versions of (21), (22) as well as (24):
Volume form of the shape derivative Let $h_{f,h} : B_h \to \mathbb{R}$, $H_{f,h} : B_h \to \mathbb{R}$ be defined by

$$\begin{aligned} h_{f,h} \;&=\; 2\frac{|\nabla_T f|^2}{f^3}(\nabla \hat{u}_h \cdot \omega_x)(\nabla \hat{p}_h \cdot \omega_x) \\ &\quad -\frac{1}{f^2}\big((\nabla_T f \cdot \nabla \hat{u}_h)(\omega_x \cdot \nabla \hat{p}_h) + (\nabla_T f \cdot \nabla \hat{p}_h)(\omega_x \cdot \nabla \hat{u}_h)\big) \\ &\quad +f\big((\hat{u}_h - \hat{z}_f)^2 - |x|(\hat{u}_h - \hat{z}_f)\nabla \hat{z}_f \cdot \omega_x - |x|\hat{F}_f\, \nabla \hat{p}_h \cdot \omega_x\big); \end{aligned} \tag{34}$$

$$\begin{aligned} H_{f,h} \;&=\; \frac{1}{f}\big((\nabla \hat{p}_h \cdot \omega_x)\nabla \hat{u}_h + (\nabla \hat{u}_h \cdot \omega_x)\nabla \hat{p}_h\big) \\ &\quad -\frac{2}{f^2}(\nabla \hat{u}_h \cdot \omega_x)(\nabla \hat{p}_h \cdot \omega_x)\, \nabla_T f. \end{aligned} \tag{35}$$

Next, let $\bar{h}_{f,h}$, $\bar{H}_{f,h} \in \mathcal{S}^N$ be given by

$$\begin{aligned} \int_0^{2\pi} \bar{h}_{f,h}(\phi)\bar{v}(\phi)\mathrm{d}\phi \;&=\; \int_{B_h} h_{f,h}(x) v(\omega_x)\,\mathrm{d}x, \quad \forall \bar{v} \in \mathcal{S}^N; \\ \int_0^{2\pi} \bar{H}_{f,h}(\phi)\bar{v}(\phi)\mathrm{d}\phi \;&=\; \int_{B_h} H_{f,h}(x) \cdot v(\omega_x)\omega_x^{\perp}\,\mathrm{d}x, \quad \forall \bar{v} \in \mathcal{S}^N, \end{aligned}$$

where, as above $v(\omega) = \bar{v}(\phi)$ if $\omega = e^{i\phi}$ and $(a_1, a_2)^{\perp} = (-a_2, a_1)$.
Boundary form of the shape derivative Let $\tilde{h}_{f,h} : \partial B_h \to \mathbb{R}$ be defined by

$$\tilde{h}_{f,h} = \frac{1}{2}(\hat{u}_h - \hat{z}_f)^2 f + \frac{1}{f}\big(1 + \frac{|\nabla_T f|^2}{f^2}\big)(\nabla \hat{u}_h \cdot \omega_h)(\nabla \hat{p}_h \cdot \omega_h),$$

where ω_h is the outer unit normal to ∂B_h. Let $\bar{h}_{f,h} \in \mathcal{S}^N$ be given by

$$\int_0^{2\pi} \bar{h}_{f,h}(\phi)\bar{v}(\phi)\mathrm{d}\phi = \int_{\partial B_h} \tilde{h}_{f,h} v(\omega_x)\mathrm{d}o_x, \quad \forall \bar{v} \in \mathcal{S}^N.$$

The functions $\bar{h}_{f,h}$ and $\bar{H}_{f,h}$ ($\bar{H}_{f,h} \equiv 0$ for the boundary form) are approximations to those that appear in the formula (25). We therefore define $I_h(\bar{f}) : \mathcal{S}^N \to \mathbb{R}$ by

$$\langle I_h(\bar{f}), \bar{v}\rangle := \int_0^{2\pi} \big(\bar{h}_{f,h}(\phi)\bar{v}(\phi) + \bar{H}_{f,h}(\phi)\bar{v}'(\phi)\big)\mathrm{d}\phi, \quad \bar{v} \in \mathcal{S}^N \tag{36}$$

as an approximation to $\langle J'(f), v\rangle$.
Based on (36) the construction of a nearly optimal descent direction $\bar{g} \in \mathcal{S}^N$ is given by one of the methods described below: a) a discrete version of the approach of Section 2.3 (see 3.2), b) an application of the Sinkhorn Algorithm from optimal transport (see 3.3), or c) a Hilbertian method (see 3.4).

Remark 3.1. *An inspection of our discrete approach yields that we also could choose the function $\bar{f} \in W^{1,\infty}(\mathbb{S}^1)$ instead of $f \in \mathcal{S}^N$, and to consider $I_h(\bar{f})$ in (36) as a linear functional on $W^{1,\infty}(\mathbb{S}^1)$, which would correspond to variational discretisation [Hin05] of our shape optimisation problem. However, the evaluation of integrals through the appearance of the functions f and $\nabla_T f$ in general requires quadrature rules. In the variational discretisation approach this could be accomplished with replacing $\bar{f}$ by its Lagrange interpolation, thus leading to the approach proposed in the present section.*

3.2. **Lipschitz formula.** Since $\bar{H}_{f,h} \in W^{1,\infty}(0, 2\pi)$ with $\bar{H}_{f,h}(0) = \bar{H}_{f,h}(2\pi)$ we may use a discrete version of the approach described in Section 2.3 in order to produce an approximate direction of steepest descent $\bar{g} \in \mathcal{S}^N$ as follows: Fix $\epsilon > 0$ and define $G \in \mathcal{S}^N$ by

$$G(\phi_i) := \bar{H}_{f,h}(0) - \bar{H}_{f,h}(\phi_i) + \int_0^{\phi_i} \left(\bar{h}_{f,h} - c\bar{f}\right)\mathrm{d}t, \qquad \text{where } c = \frac{\int_0^{2\pi} \bar{h}_{f,h}\mathrm{d}t}{\int_0^{2\pi} \bar{f}\mathrm{d}t}.$$

For $i = 1, \ldots, N$ and $G_i = G(\phi_i)$ we let

$$\begin{aligned} M_i &:= \sum_{j=1}^{N} \frac{2\pi}{N} \chi_{G_j \le G_i}, \quad \beta := \max\{G_i : M_i < \pi : i = 1, ..., N\}; \\ O_\pm &:= \{i \in \{1, \ldots, N\} : G_i \gtrless \beta \pm \epsilon\}, \, O_0 := \{1, \ldots, N\} \setminus (O_+ \cup O_-), \\ k &:= \begin{cases} 0, & O_0 = \emptyset, \\ \frac{|O_+| - |O_-|}{|O_0|}, & \text{otherwise.} \end{cases} \end{aligned}$$

Finally, let $\tilde{g} \in \mathcal{S}^N$ be defined by

$$\tilde{g}(\phi_i) = \frac{1}{2}\frac{2\pi}{N} \sum_{j=1}^{i} \chi_{j \in O_-} + \chi_{j-1 \in O_-} - \chi_{j \in O_+} - \chi_{j-1 \in O_+} + k\left(\chi_{j \in O_0} + \chi_{j-1 \in O_0}\right). \tag{37}$$

Motivated by Propostion 2.5 our approximate steepest descent direction $\bar{g} \in \mathcal{S}^N$ is then given by

$$\bar{g} = -\tilde{g} + \frac{1}{2\pi} \int_0^{2\pi} \bar{f}\tilde{g}\mathrm{d}\phi. \tag{38}$$

We now make some remarks on this discretisation:

- The sets O_+, O_- and O_0 are not necessarily the natural discrete version of their counterparts in (29), this is chosen to avoid the need to find the points which are identically equal to β and allow us to give the function $\tilde{g}$ as a discrete function in $\mathcal{S}^N$.
- It may be preferable to choose the $\epsilon > 0$ to depend on the discretisation and current state. For our experiments we take
$$\epsilon = \frac{3}{2N}\left(\max_{i=1,\ldots,N} G_i - \min_{i=1,\ldots,N} G_i\right)$$

3.3. **Sinkhorn algorithm.** Motivated by Remark 2.4, the appropriate problem is the transport of mass from the measure $(\bar{h}_f - \bar{H}_f' - c\bar{f})^+\mathrm{d}\phi$ to the measure $(\bar{h}_f - \bar{H}_f' - c\bar{f})^-\mathrm{d}\phi$, where the cost of transportation of mass between two points is given by the intrinsic distance, i.e.

$$d(\phi, \tilde{\phi}) = \arccos(\cos(\phi - \tilde{\phi})), \quad \phi, \tilde{\phi} \in [0, 2\pi].$$

In order to discretise this transport problem we abbreviate $q_{f,h} := \bar{h}_{f,h} - \bar{H}'_{f,h} - c\bar{f}$ and approximate the measures $q^+_{f,h}\mathrm{d}\phi$ and $q^-_{f,h}\mathrm{d}\phi$ by atoms with appropriate strictly positive weights as follows. Denoting by $\{\varphi_1, \ldots, \varphi_N\}$ the standard nodal basis of $\mathcal{S}^N$ we set

$$a_i := \int_0^{2\pi} q_{f,h}\varphi_i \mathrm{d}\phi, \quad i = 1, \ldots, N$$

as well as $N^\pm := \{i \in \{1, \ldots, N\} \,|\, a_i \gtrless 0\}$. Then, $\sum_{i\in N^+} a_i \delta_{\phi_i}$ approximates the measure $q^+_{f,h}\mathrm{d}\phi$, while $\sum_{j\in N^-}(-a_j)\delta_{\phi_j}$ is an approximation of $q^-_{f,h}\mathrm{d}\phi$. With this, the discrete optimal transport problem is to find $P \in \mathbb{R}_+^{|N^+|\times|N^-|}$ which maximises

$$\sum_{i\in N^+}\sum_{j\in N^-} C_{ij}P_{ij},$$

subject to $\sum_{j\in N^-} P_{ij} = a_i, i \in N^+$ and $\sum_{i\in N^+} P_{ij} = -a_j, j \in N^-$, where $C_{ij} = d(\phi_i, \phi_j)$. We will use the Sinkhorn algorithm to approximate a minimiser. For $\delta > 0$, the Sinkhorn algorithm minimises the regularised quantity

$$\sum_{i\in N^+}\sum_{j\in N^-} C_{ij}P_{ij} + \delta P_{ij}(\log(P_{ij}) - 1).$$

Letting $K_{ij} = \exp(-\frac{1}{\delta}C_{ij})$, $u_i^0 = 1$ and $v_j^0 = 0$ for $i \in N^+$, $j \in N^-$, the Sinkhorn iteration is given by

$$u_i^{l+1} = \frac{a_i}{(Kv^l)_i}, i \in N^+, \quad v_j^{l+1} = \frac{-a_j}{(K^T u^{l+1})_j}, j \in N^-$$

for $l \geq 0$. The vectors $(\delta\log(u_i^l))_{i\in N^+}$ and $(\delta\log(v_j^l))_{j\in N^-}$ are the dual variables in this iteration.

We set $\delta = 0.05$ and stop the iterations when either $l = 2000$ or $\frac{1}{|N^+|}\sum_{i\in N^+}|a_i - \sum_{j\in N^-} u_i^l K_{ij} v_j^l| \leq 10^{-6}$ and $\frac{1}{|N^-|}\sum_{j\in N^-}|-a_j - \sum_{i\in N^+} u_i^l K_{ij} v_j^l| \leq 10^{-6}$. We finally define $\bar{g} \in \mathcal{S}^N$ by assigning the following values at the vertices ϕ_i:

$$\begin{aligned}
\bar{g}(\phi_i) &= \inf_{j\in N^-}\left(-\delta\log(v_j^l) + C_{ij}\right), \quad i \in N^+, \\
\bar{g}(\phi_j) &= \sup_{i\in N^+}\left(\bar{g}(\phi_i) - C_{ij}\right), \quad j \in N^-, \\
\bar{g}(\phi_i) &= \inf_{j\in N^-}\left(-\delta\log(v_j^l) + d(\phi_i, \phi_j)\right), \quad i \in \{1, \ldots, N\} \setminus (N^+ \cup N^-).
\end{aligned}$$

It is again necessary to remove a constant to ensure that $\int_0^{2\pi} \bar{f}\bar{g}\mathrm{d}\phi = 0$. We note that this method to assign $\bar{g}$ at the vertices is not the typical way to identify the dual variable in the Sinkhorn algorithm, however it was found to give preferable results for $\bar{g}$ both in terms of the shape and of the evaluation of $\int_0^{2\pi} q_{f,h}\bar{g}\mathrm{d}\phi$.

3.4. H^1 **minimising direction.** According to [IL05, Theorem 2.1], our Lipschitz direction $\bar{g}$ from Proposition 2.5 can be obtained as the uniform p-limit of the rescaled minimisers v^* of

$$v \in \mathcal{S}^N \mapsto \int_0^{2\pi} \frac{1}{p}|v'|^p + \bar{h}_f v + \bar{H}_f v' \mathrm{d}\phi$$

such that $\int_0^{2\pi} v\bar{f} = 0$, where we rescale $\bar{g}_p := \frac{v^*}{\|(v^*)'\|_{L^p(0,2\pi)}}$. The rescaling is done so that $\bar{g}_p$ is a direction in the topology induced by the $W^{1,p}$-seminorm. In this setting the approaches commonly used in the literature so far correspond to the Hilbert space case $p = 2$, see [ADJ21, Section 5.2] for a detailed discussion, and also [EH12; HSUar; HPS15; Sch+13; SSW15; SSW16; SW17], which we here consider as a reference case for comparison of our approach.

4. Numerical Experiments

The numerical experiments carried out in this section combine the following Armijo–type descent method with one of the choices for a descent direction described in the previous section:

Algorithm 1: Our implemented Armijo algorithm

```
Given f̄ ∈ S^N;
Solve for û_h;
Set E = 1/2 ∫_{B_h} (û_h − ẑ_f)^2 f^2;
for j = 1, ..., maxIt do
    Solve for p̂_h;
    Construct descent ḡ;
    set fOld = f̄;
    for σ ∈ {1/16, 1/32, 1/64, ...}, and σ ≥ 10^{-8} do
        Set f̄ = fOld + σḡ;
        Solve for û_h;
        if 1/2 ∫_{B_h} (û_h − ẑ_f)^2 f^2 < E + 10^{-5} σ⟨I_h(f̄), ḡ⟩ then
            set E = 1/2 ∫_{B_h} (û_h − ẑ_f)^2;
            break;
```

We set $\mathrm{maxIt} = 250$, we will also terminate the algorithm if we require $\sigma < 10^{-8}$. In our numerical implementation, whenever we set f, we rescale it to have the same square integral as the original domain. The images of the grids are created with ParaView [Aya15] and our finite element methods for state and costate equations are performed with DUNE [Bla+16]. The boundary has discretisation with $N = 512$ and the triangulation B_h is shown in Figure 1.

In order to plot the graphs for the energy throughout the iterations of the experiments in a meaningful way we use a log scale. When the energy is not expected to vanish, as in the experiments in Sections 4.0.1 and 4.0.2, we take away lowest energy value attained by any of the experiments from all of the data, this value appears in the y axis label of the graphs.

4.0.1. *An experiment with $F = 0$.* For this experiment, we set $F(x_1, x_2) = 0$ and $z(x_1, x_2) = |x_1 + x_2| + |x_1 - x_2|$. Since $F = 0$ it follows that $u = 0$, therefore when considering the boundary form of the shape derivative which appears in (16), we see that when the boundary of the domain is in a level-set of z^2, the energy will be critical. When starting with $f = 1$, we expect the final domain to be the square $\left(-\frac{\sqrt{\pi}}{2}, \frac{\sqrt{\pi}}{2}\right)^2$. After 250 iterations, the method with optimal transport direction with boundary form of derivative gives the domain on the left of Figure 2. The method using the Lipschitz formula with boundary form of derivative terminated after 103 iterations, the domain at this point is given in the middle of Figure 2.

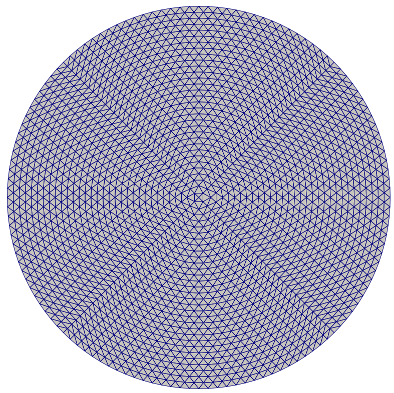

FIGURE 1. Triangulation of the computational domain.

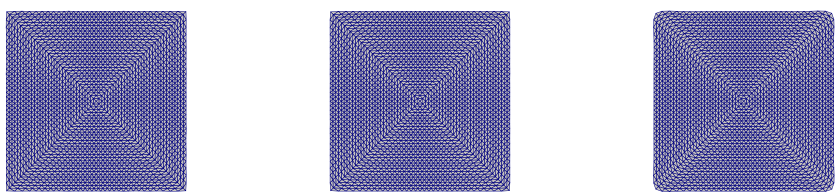

FIGURE 2. Final domains for the experiment in Section 4.0.1 with Lipschitz optimal transport descent (left), Lipschitz formula descent (middle) and H^1 descent (right).

The result of 250 iterations of the H^1 method is given on the right of Figure 2. A graph of energy throughout the iterations is given in Figure 3.

The Lipschitz formula method with boundary form terminated after 103 steps because it had achieved very close to the shape we expected to be minimal. Whereas the Lipschitz formula method with volume form terminated after only 18 steps, possibly related to a poor choice of parameters. For the Lipschitz optimal transport method with volume form of derivative terminated after 121 steps, where we see that this energy has already become very low. One may see that the corners from the Lipschitz methods are highly developed, whereas they are rather curved for the H^1 method, this is highlighted in Figure 4 which gives in a zoom in of the corners of Figure 2.

4.0.2. *An experiment with $-\Delta z = 4F$.* For this experiment we set $F(x_1, x_2) = 1$ and $z(x_1, x_2) = 1 - x_1^2 - x_2^2$. We notice that $-\Delta z = 4F$ and that z vanishes on the unit ball. We start this experiment with f representing the square $\left(-\frac{\sqrt{\pi}}{2}, \frac{\sqrt{\pi}}{2}\right)^2$, which is shown in Figure 5.

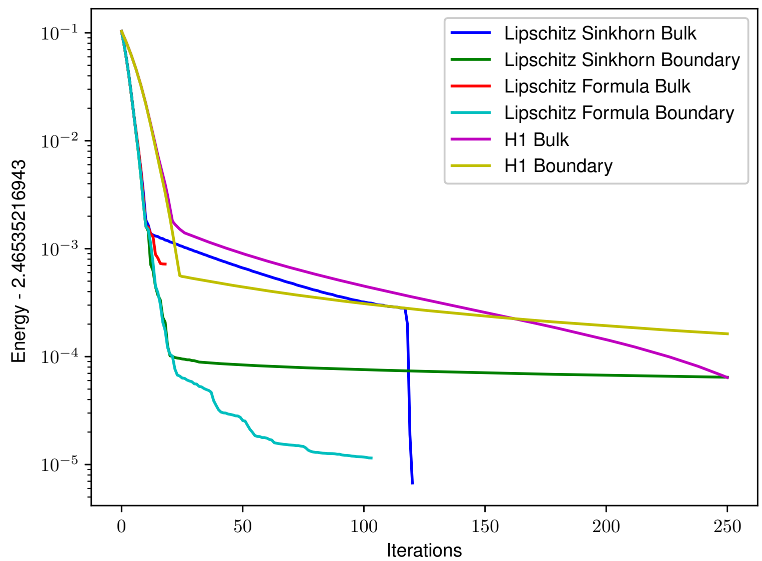

FIGURE 3. Graph of the energy for the iterates in the experiment in Section 4.0.1

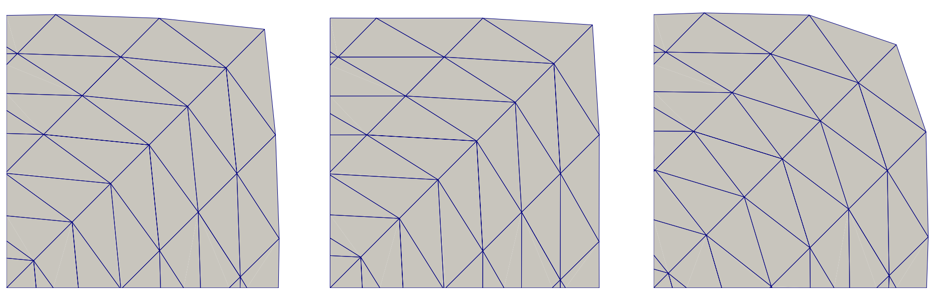

FIGURE 4. Zoom in on the top right 'corners' of the final domains for the experiment in Section 4.0.1 with Lipschitz optimal transport descent (left), Lipschitz formula descent (middle) and H^1 descent (right).

In this experiment we provide the domain after 15 iterations, this appears in Figure 6. We provide this as such comparisons are of interest in practical applications, where computation time is a limiting factor. We see that even after only 15 iterations that the shapes are close to a circle, with the Lipschitz methods outperforming the H^1 methods significantly.

After 250 iterations, the Lipschitz optimal transport method with volume form of the shape derivative gives the domain on the left of Figure 7. The H^1 method with volume form of shape derivative terminated after 31 iterations and the domain at this point is shown on the right of Figure 7. A graph of energy throughout the

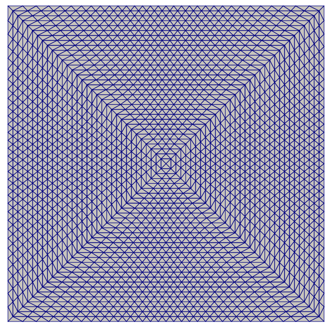

FIGURE 5. Initial domain for the experiment in Section 4.0.2.

iterations is given in Figure 8. We note that both of the H^1 methods terminate early, the boundary method after 110 iterations and the volume method after 31. We suggest that this termination happens because they are struggling to remove the corners. We also see that both of the Lipschitz methods with the boundary form of the shape derivative terminate early, the method with formula after 28 steps and the optimal transport method after 14. One might attribute this to the Lipschitz methods are struggling with the boundary form of shape derivative.

It is seen that the corners appearing in the H^1 method, which are artefacts of the original grid, cause difficulties for the H^1 method, whereas the Lipschitz methods were able to remove them. These artefact corners also make an appearance in [HP15, Figure 2] when starting with an initial guess of a square and target of a circle.

4.0.3. *An experiment with* $-\Delta z = F$. For this experiment we set $F(x_1, x_2) = 16\pi - 32x_1^2 - 32x_2^2$ and $z(x_1, x_2) = (\pi - 4x_1^2)(\pi - 4x_2^2)$. We notice that $-\Delta z = F$ and that $z(x_1, \pm\sqrt{\pi}/2) = z(\pm\sqrt{\pi}/2, x_2) = 0$ for all $x_1, x_2 \in \mathbb{R}$. An immediate consequence of these facts is that there is a domain which attains zero energy, the square $\left(-\frac{\sqrt{\pi}}{2}, \frac{\sqrt{\pi}}{2}\right)^2$. The experiment is started with $f = 1$. After 250 iterations, the Lipschitz optimal transport method method with volume form of shape derivative gives the domain on the left of Figure 9 and after 250 iterations the H^1 method with volume form of shape derivative gives the domain on the right of Figure 9.

A graph of energy throughout the iterations is given in Figure 10. It is seen that the method using the Lipschitz method with formula with the boundary form of the derivative terminates early, after 19 iterations. We note that this method, despite early termination, has a lower energy than all but one other method and we attribute the early termination to the fact that its energy has become so low.

Here we see that none of the methods perform particularly well, however it is clear that the Lipschitz methods are outperforming the H^1 methods in terms of energy minimisation and in terms of the sharpness of the corners.

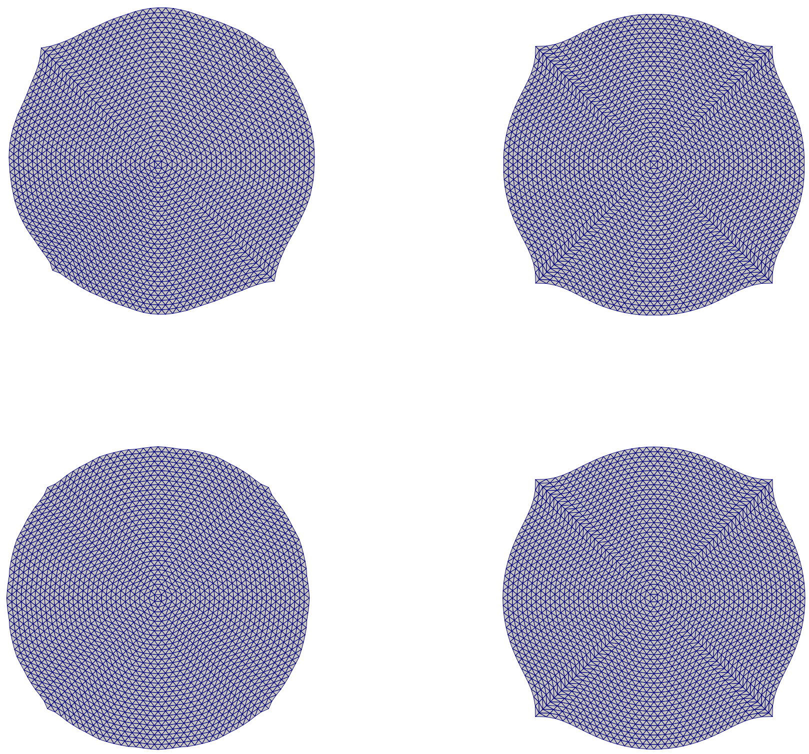

FIGURE 6. Domains after 15 iterations for the experiment in Section 4.0.2 with Lipschitz formula descent (left) and H^1 descent (right) with the volume form (top) of the shape derivative and the boundary form (bottom).

4.0.4. *An experiment with known minimum which is not a Lipschitz domain.* For this experiment we set $F(x_1, x_2) = 1$ and

$$z(x_1, x_2) = \frac{1}{8} - \frac{1}{4}\min\left(\left(x_1 - \frac{1}{\sqrt{2}}\right)^2, \left(x_1 + \frac{1}{\sqrt{2}}\right)^2\right) - \frac{1}{4}x_2^2.$$

We see that away from $x_1 = 0$, $-\Delta z = F$. Therefore it is expected that the double ball, $B(y_+, \frac{1}{\sqrt{2}}) \cup B(y_-, \frac{1}{\sqrt{2}})$ for $y_\pm = (\pm\frac{1}{\sqrt{2}}, 0)^T$ is a minimising domain. Notice that this double ball is not a Lipschitz domain and that the f which represents the domain has zeroes. After 73 iterations, the Lipschitz formula method with volume form of the derivative gives the domain on the left of Figure 11 and the H^1 method with volume form of the shape derivative gives the domain on the right of Figure 11.

A graph of energy throughout the iterations is given in Figure 12. We note

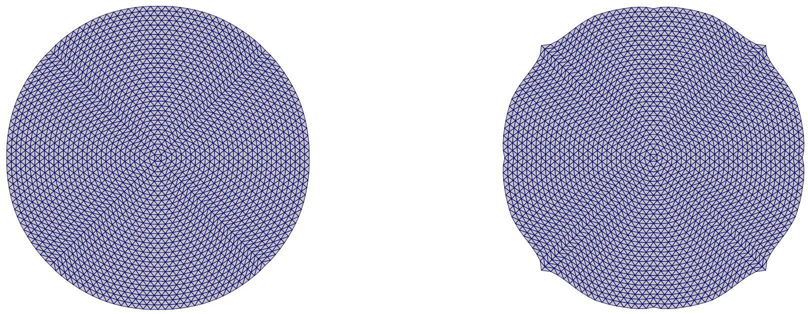

FIGURE 7. Final domains for the experiment in Section 4.0.2 with Lipschitz optimal transport descent (left) and H^1 descent (right) with the volume form of the shape derivative.

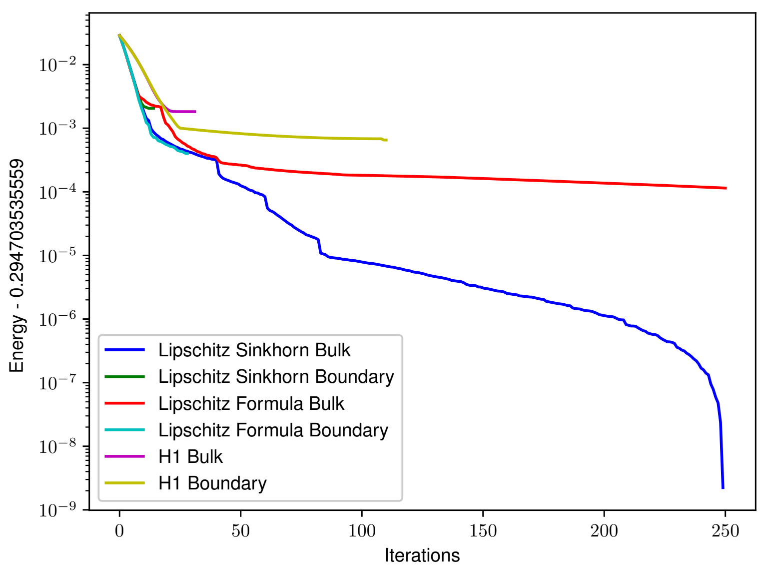

FIGURE 8. Graph of the energy for the iterates in the experiment in Section 4.0.2

that the Lipschitz formula method with volume form of derivative terminates after 73 iterations, where one might attribute this to how close to the optimal shape it appears to have attained.

We see that both methods seem to cope relatively well. The Lipschitz method appears to perform much better at forming the cusp and the domain appears more circular. We note that it is also possible to (under certain regularity conditions)

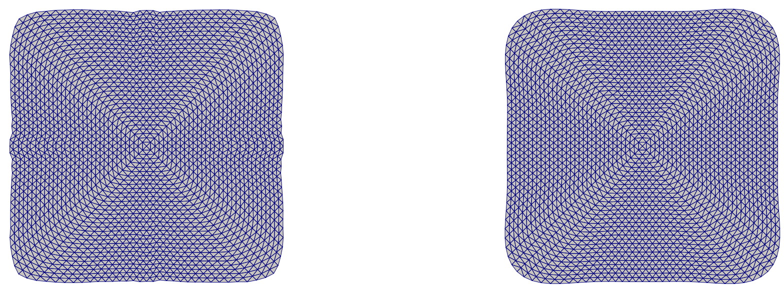

FIGURE 9. Final domains for the experiment in Section 4.0.3 with Lipschitz optimal transport descent (left) and H^1 descent (right) with the volume form of the shape derivative.

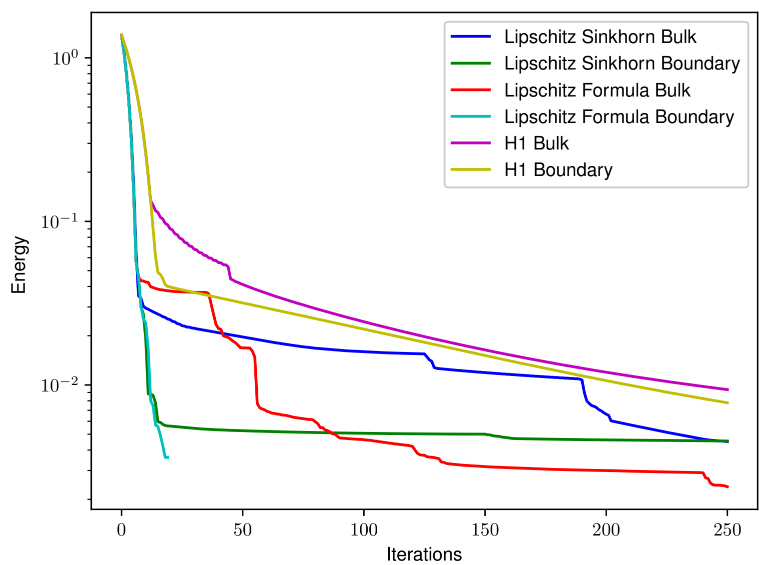

FIGURE 10. Graph of the energy for the iterates in the experiment in Section 4.0.3

consider an analogous direction of maximal descent over Hölder functions, rather than Lipschitz functions, this is done in [Jyl15].

4.1. **Comments on experiments.** Over all of the experiments, we see that the Lipschitz methods outperform the H^1 method. Regularly the formula approach appears better than the optimal transport method, but lacks the capability to be

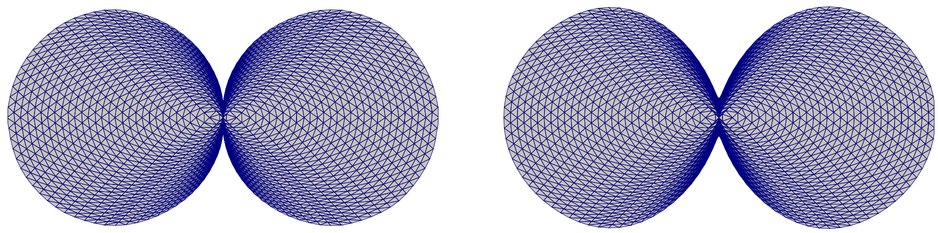

FIGURE 11. Final domains for the experiment in Section 4.0.4 with Lipschitz formula descent (left) and H^1 descent (right) with the volume form of the shape derivative.

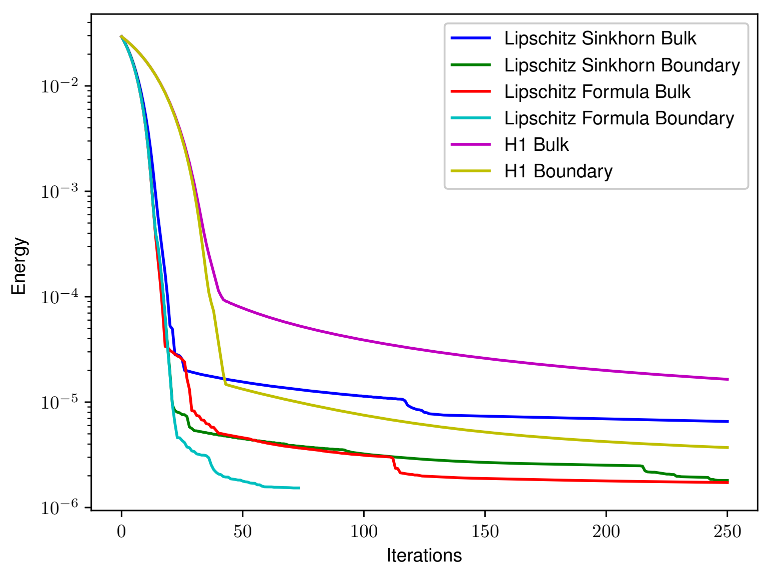

FIGURE 12. Graph of the energy for the iterates in the experiment in Section 4.0.4

generalised to higher dimensions. We also note that the formula is significantly quicker to arrive at the direction (in a very naive sequential implementation). We note that many more algorithms for solving the optimal transport are available and perhaps others may be better suited to this problem. For the moment we note that the Sinkhorn algorithm experiences very efficient speedup from parallel processing.

5. Conclusion

In this article we introduce a novel method for the implementation of shape optimsiation with Lipschitz domains. We propose to use the shape derivative to determine deformation fields which represent steepest descent directions of the shape functional in the $W^{1,\infty}$ topology. The idea of our approach is demonstrated for shape optimisation of 2-dimensional star-shaped domains. We also highlight the connections to optimal transport, for which discretisation methods are available. We present several numerical experiments illustrating that our approach seems to be superior over existing Hilbert space methods, in particular in developing optimal shapes with corners and in providing a quicker energy descent.

Acknowledgements

This work is part of the project P8 of the German Research Foundation Priority Programme 1962, whose support is gratefully acknowledged by the second and the third author.

References

[ADJ21] G. Allaire, C. Dapogny, and F. Jouve. "Shape and topology optimization". In: *Differential Geometric Partial Differential Equations: Part II.* Vol. 22. Handbook of Numerical Analysis. Amsterdam, Netherlands: Elsevier, 2021, pp. 3–124.

[Aya15] U. Ayachit. *The ParaView Guide: A Parallel Visualization Application.* Clifton Park, NY, USA: Kitware, Inc., 2015.

[Bel+97] J. A. Bello, E. Fernández-Cara, J. Lemoine, and J. Simon. "The Differentiability of the Drag with Respect to the Variations of a Lipschitz Domain in a Navier–Stokes Flow". In: *SIAM Journal on Control and Optimization* 35.2 (1997), pp. 626–640.

[Bla+16] M. Blatt, A. Burchardt, A. Dedner, C. Engwer, J. Fahlke, B. Flemisch, C. Gersbacher, C. Gräser, F. Gruber, C. Grüninger, D. Kempf, R. Klöfkorn, T. Malkmus, S. Müthing, M. Nolte, M. Piatkowski, and O. Sander. "The Distributed and Unified Numerics Environment, Version 2.4". In: *Archive of Numerical Software* 4.100 (2016), pp. 13–29.

[Bra+15] C. Brandenburg, F. Lindemann, M. Ulbrich, and S. Ulbrich. "A Continuous Adjoint Approach to Shape Optimization for Navier Stokes Flow." In: *Optimal Control of Coupled Systems of Partial Differential Equations.* Vol. 158. Int. Ser. Numer. Math. Basel: Birkhäuser, 2015, pp. 35–56.

[Bur98] V. I. Burenkov. *Sobolev spaces on domains.* Vol. 137. Springer, 1998.

[DDE05] K. Deckelnick, G. Dziuk, and C. M. Elliott. "Computation of geometric partial differential equations and mean curvature flow". In: *Acta Numerica* 14 (2005), pp. 139–232.

[DZ01] M. C. Delfour and J.-P. Zolésio. *Shapes and Geometries: Analysis, Differential Calculus, and Optimization.* USA: Society for Industrial and Applied Mathematics, 2001.

[EH12] K. Eppler and H. Harbrecht. “Shape optimization for free boundary problems”. In: *Proceedings of the International Conference Systems Theory: Modelling, Analysis and Control*. Vol. 160. Internat. Ser. Numer. Math. basel: Birkhäuser, 2012, pp. 277–288.

[Fis+17] M. Fischer, F. Lindemann, M. Ulbrich, and S. Ulbrich. “Fréchet Differentiability of Unsteady Incompressible Navier–Stokes Flow with Respect to Domain Variations of Low Regularity by Using a General Analytical Framework”. In: *SIAM Journal on Control and Optimization* 55.5 (2017), pp. 3226–3257.

[Gar+15] H. Garcke, C. Hecht, M. Hinze, and C. Kahle. “Numerical approximation of phase field based shape and topology optimization for fluids”. In: *SIAM J. Sci. Comput.* 37 (2015), A1846–A1871.

[Gar+18] H. Garcke, M. Hinze, C. Kahle, and K. Lam. “A phase field approach to shape optimization in Navier- Stokes flow with integral state constraints”. In: *Adv. Comput. Math.* 44 (2018), pp. 1345–1383.

[GM94] P. Guillaume and M. Masmoudi. “Computation of high order derivatives in optimal shape design”. In: *Numerische Mathematik* 67.2 (1994), pp. 231–250.

[Hin05] M. Hinze. “A variational discretization concept in control constrained optimization: the linear-quadratic case”. In: *Comput. Optim. Appl.* 30 (2005), pp. 45–63.

[HP15] R. Hiptmair and A. Paganini. “Shape optimization by pursuing diffeomorphisms”. In: *Computational Methods in Applied Mathematics* 15.3 (2015), pp. 291–305.

[HPS15] R. Hiptmair, A. Paganini, and S. Sargheini. “Comparison of approximate shape gradients”. In: *BIT Numerical Mathematics* 55.2 (2015), pp. 459–485.

[HSUar] J. Haubner, M. Siebenborn, and M. Ulbrich. “A Continuous Perspective on Shape Optimization Via Domain Transformations”. In: *Siam J. Sci. Comput.* (2021, to appear).

[HUU20] J. Haubner, M. Ulbrich, and S. Ulbrich. “Analysis of shape optimization problems for unsteady fluid-structure interaction”. In: *Inverse Problems* 36 (2020), pp. 1–38.

[IL05] H. Ishii and P. Loreti. “Limits of solutions of p-Laplace equations as p goes to infinity and related variational problems”. In: *SIAM journal on mathematical analysis* 37.2 (2005), pp. 411–437.

[Jyl15] H. Jylhä. “An optimal transportation problem related to the limits of solutions of local and nonlocal p-Laplace-type problems”. In: *Revista matemática complutense* 28.1 (2015), pp. 85–121.

[Küh+19] N. Kühl, P. Müller, M. Hinze, and T. Rung. “Decoupling of Control and Force Objective in Adjoint-Based Fluid Dynamic Shape Optimization”. In: *AIAA Journal* 57 (2019), p. 4110.

[MS76] F. Murat and J. Simon. “Etude de problemes d’optimal design”. In: *Optimization Techniques Modeling and Optimization in the Service of Man Part 2*. Berlin, Heidelberg: Springer Berlin Heidelberg, 1976, pp. 54–62.

[Rad+18] L. Radke, J. Heners, M. Hinze, and A. Düster. “A partitioned approach for adjoint shape optimization in fluid-structure interaction”. In: *J. Comput. Mech.* 61 (2018), pp. 259–276.

[San15] F. Santambrogio. "Optimal transport for applied mathematicians". In: *Birkäuser, NY* 55.58-63 (2015), p. 94.

[Sch+13] S. Schmidt, C. Ilic, V. Schulz, and N. Gauger. "Three dimensional large scale aerodynamic shape optimization based on the shape calculus". In: *AIAA Journal* 51 (2013), pp. 2615–2627.

[Sim80] J. Simon. "Differentiation with respect to the domain in boundary value problems". In: *Numerical Functional Analysis and Optimization* 2.7-8 (1980), pp. 649–687.

[SSW15] V. Schulz, M. Siebenborn, and K. Welker. "PDE constrained shape optimization as optimization on shape manifolds". In: *Geometric Science of Information*. Vol. 9389. Lecture Notes in Computer Science. New York: Springer, 2015, pp. 499–508.

[SSW16] V. Schulz, M. Siebenborn, and K. Welker. "Efficient PDE constrained shape optimization based on Steklov-Poincaré type metrics". In: *Siam J. Optim.* 26 (2016), pp. 2800–2819.

[SW17] M. Siebenborn and K. Welker. "Algorithmic Aspects of Multigrid Methods for Optimization in Shape Spaces". In: *Siam J. Sci. Comput.* 39.6 (2017), B1156–B1177.

[SZ92] J. Sokołowski and J. Zolésio. *Introduction to Shape Optimization: Shape Sensitivity Analysis*. Lecture Notes in Computer Science. Springer-Verlag, 1992.